DOI: 10.24850/j-tyca-2022-04-06

Articles

Morphometric and hydrogeochemical weighting methodology to classify susceptibility to chemical weathering in the sub-basins of the Caplina River, Tacna, Peru

Metodología de ponderación morfométrica e hidrogeoquímica para clasificar la susceptibilidad a la meteorización química en las subcuencas del río Caplina, Tacna, Perú

Alissa Vera[1], ORCID: https://orcid.org/0000-0003-0939-6315

Mahendra P. Verma[2], ORCID: https://orcid.org/0000-0001-6559-7184

Edwin Pino-Vargas[3], ORCID: https://orcid.org/0000-0001-7432-4364

German Huayna[4], ORCID: https://orcid.org/0000-0002-4518-1023

[1]Universidad Nacional Jorge Basadre Grohmann, Tacna, Perú, averam@unjbg.edu.pe

[2]Instituto Nacional de Electricidad y Energías Limpias, Cuernavaca, Morelos, Mexico / Universidad Politécnica de Nochixtlán "Abraham Castellanos", Carretera a San Mateo Etlatongo km. 2.5, Asunción Nochixtlán, Oaxaca, México, mpv55.mx1@gmail.com

[3]Universidad Nacional Jorge Basadre Grohmann, Tacna, Perú, epinov@unjbg.edu.pe

[4]Universidad Nacional Jorge Basadre Grohmann, Tacna, Perú, ghuaynaf@unjbg.edu.pe

Corresponding author: Alissa Vera, averam@unjbg.edu.pe

Abstract

A heuristic weighting methodology is formulated to classify the susceptibility to chemical weathering in the Caplina basin from two approaches: hydrogeochemical and geological morphometric. The main objective was to study the hydrological recharge of an arid basin with differential chemical weathering of geological formations in contact due to the salinization of water flow.

The parameters in the morphometric approach were analyzed in two proposed indices: (1) historical reload, from the parameters of shape and hypsometric curve; (2) runoff speed with low slopes (3-12 %), drainage density < 0.8 km^{-1}. According to their morphometry, the Caplina and Magollo sub-basins are more susceptible to chemical weathering in the Caplina basin.

For the validation of the methodology, the inventory of hydrochemical samples of the Peruvian Geological Service (Ingemmet) was used. The resulting classification of weights determined about 80 % of underground and surface sources in the basin are predominantly salinized in hydrogeological units of high and medium susceptibility to weathering. The final map generated at a scale of 1:500 000 identifies two hydrogeological units with high susceptibility to weathering: (1) fissured aquifers with hydrothermal alteration, in the Chachacumane, Chulluncane, Huilacollo, Volcánico Barroso formations, contributing calcium sulfate trends in 41.2 % of the total samples; (2) intrusive aquitards, in the Yarabamba and Challaviento formations, which influence the oxidation of sulfides in the hydrochemistry of 17.6 % of the samples. Likewise, aquitards of the volcanic origin of medium susceptibility to weathering are identified, with a considerable sodium contribution in 20.6 % of the study samples.

Keywords: Chemical weathering, susceptibility, salinization, weightings, morphometry, hydrogeology, and hydrogeochemistry.

Resumen

Se formula una metodología de ponderación heurística para clasificar la susceptibilidad a la meteorización química en la cuenca del Caplina desde dos enfoques: hidrogeoquímico y geológico morfométrico. El objetivo principal fue estudiar la recarga hidrológica de una cuenca árida con meteorización química diferencial de formaciones geológicas en contacto debido a la salinización del flujo de agua.

Los parámetros en el enfoque morfométrico se analizaron en dos índices propuestos: (1) recarga histórica, a partir de los parámetros de forma y curva hipsométrica; (2) velocidad de escurrimiento en pendientes bajas (3-12 %), con densidad de drenaje < 0.8 km^{-1}. Según su morfometría, las subcuencas Caplina y Magollo son más susceptibles a la meteorización química en la cuenca Caplina. Se interrelacionó la geoquímica (litología, minerales alterables y presencia de alteración hidrotermal) e hidrogeología (porosidad y permeabilidad).

Para la validación de la metodología se utilizó el inventario de muestras hidroquímicas del Servicio Geológico Peruano (Ingemmet) y la clasificación resultante de ponderaciones determinó 80 % de fuentes subterráneas y superficiales en la cuenca están salinizadas predominantemente en unidades hidrogeológicas de alta y media susceptibilidad a la meteorización. El mapa final generado a escala 1:500 000 identifica dichas unidades hidrogeológicas: (1) acuíferos fisurados con alteración hidrotermal en las formaciones Chachacumane, Chulluncane, Huilacollo, Volcánico Barroso, aportando tendencias cálcicas sulfatadas en el 41.2 % del total de muestras; (2) acuitardos intrusivos en las formaciones Yarabamba y Challaviento, que influyen en oxidación de sulfuros en la hidroquímica del 17.6 % de muestras. Asimismo, se identifican los acuitardos de origen volcánico de susceptibilidad media a la meteorización, con un considerable aporte sódico en el 20.6 % de muestras del estudio.

Palabras clave: meteorización química, susceptibilidad, salinización, ponderación, morfometría, hidrogeología e hidrogeoquimica.

Received: 26/10/2020

Accepted: 09/06/2021

Introduction

The current state of knowledge leads to interrelating the topography and drainage of rivers and the mineralogical and geochemical texture of the transport of sediments, which experience weathering in basins variable to climatic conditions (Kanhaiya, Singh, Singh, Mittal, & Srivastava, 2019). The mass balance based on the cation calculation by Li, Han, Liu, Yang, and Liu (2019) shows that weathering by silicates, carbonates, atmospheric contributions, and anthropogenic factors contribute to the dissolved load in river water. This natural increase is also attributable to transport through lithologies of particular mineralogical composition, the temperature of the geological medium, contact time, and length of travel (Custodio & Llamas, 1983; Molina, 2005). Likewise, the mixing process of groundwater, meteoric, and glacier water puts footprints of the seasonal variation in the hydrochemistry of the basins (Ansari, Ahmad, & Khan, 2019).

The Caplina basin corresponds to a hydrographic unit on the Pacific slope in Southern Peru. The salinization process in the surface and underground water of the basin exposes an excess of heavy chemical elements such as As, Hg, and Pb in its primary channel (Pino *et al*., 2017; ANA, 2011). Hydrothermal emanations generate geogenic contamination in the NE of the basin identified as a recharge zone (Pino *et al*., 2017; Pino, Montalván, Vera, & Ramos, 2019[a]).

In Figure 1, the basin's location is observed at the head of the Atacama desert, in the extreme South of Peru and north of Chile. This region has a hyper-arid climate, and its hyper aridity is attributed to its subtropical location (Pino, Ramos, Mejía, Chávarri, & Ascensios, 2020; Pino *et al*., 2019a; Pino *et al*., 2019b; Pino, 2019; Pino, Chávarri, & Ramos, 2018; Pino *et al*., 2017; Garreaud, Molina, & Farias, 2010; Garreaud, Vuille, & Clement, 2003) and, therefore, there exists a slow hydrological recharge (Foster, Tuinhof, Kemper, Garduno, & Nanni, 2003; Narvaez-Montoya *et al*., 2022). The low flow velocity predisposes the chemical reactions in the water-rock contact and induces some erosion of sediments. The water-rock interaction becomes the leading salinizing agent; therefore, sediment erosion is not considered in the present case study.

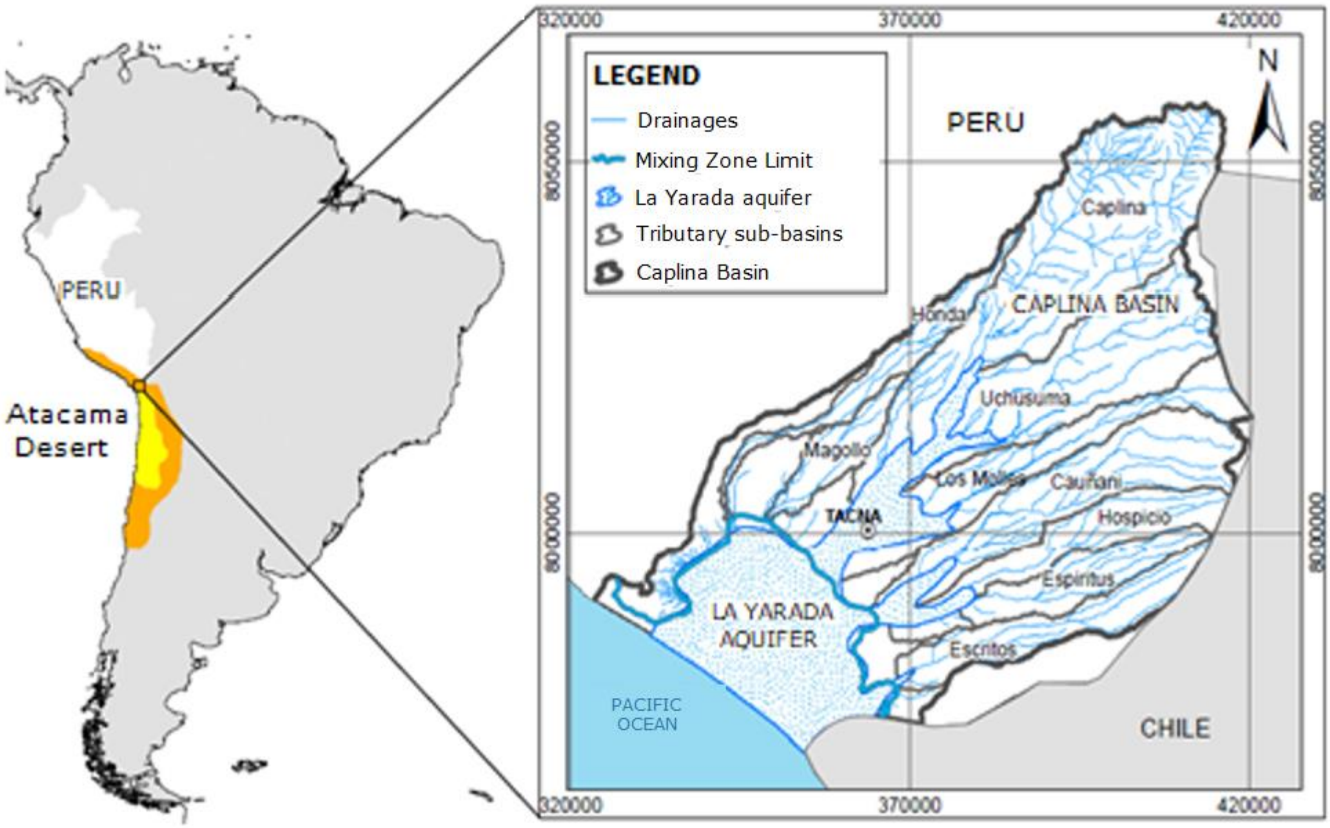

Figure 1. Location of the Caplina river basin in the Atacama Desert and its division into nine sub-basins.

The geogenic contamination and arid climate are associated with the natural salinization in the sub-basins of the Caplina River. The present study aims to formulate a heuristic methodology to classify the susceptibility to chemical weathering in the Caplina basin from two approaches: morphometric and hydrogeochemical.

The heuristic method weights variables to estimate vulnerability and susceptibility; applied in quantifying the danger of soil erosion, proposed by Rajbanshi and Bhattacharya (2020) and Adhami and Hamidreza (2016) with spatial prioritization of the sub-basins. Additionally, Manfreda *et al*. (2014) weighed three geomorphic approaches for identifying flood-prone areas and evaluating susceptibility to mass movements (Secretaría de Gestión de Riesgos, 2015). Thus, the weighting mechanism is principally formulated on the morphometric, hydrogeological, and hydrogeochemical analysis against the salinization process of the flow by chemical weathering in the Caplina basin.

Materials and methods

Adhami and Hamidreza (2016) determined five independent factors in sediment performance: physiographic, geological, climatic, land use, and hydrological. Pacheco and Van der Weijden (Pacheco & Van der Weijden,

Tecnología y Ciencias del Agua

OPEN ACCESS

Check for updates

2012; Pacheco & Van der Weijden, 2014; Chucuya, S.; Vera, A.; Pino-Vargas, E.; Steenken, A.; Mahlknecht, J.; Montalván, I. Hydrogeochemical Characterization and Identification of Factors Influencing Groundwater Quality in Coastal Aquifers, Case: La Yarada, Tacna, Peru. Int. J. Environ. Res. Public Health 2022, 19, 2815. https://doi.org/10.3390/ijerph19052815 proposed a weathering algorithm that integrates topographic, hydrological, rock structure, and chemical data to calculate basin-scale weathering rates.

Considering the above factors, the weighing approaches of the Caplina basin were: morphometric and geological. Bransford and Stein (1987) proposed a morphometric heuristic method and described empirical rules to evaluate the effects of an activity.

Hydrological characterization

Rainfall recharge in the Caplina basin has been low for several decades (Motta-Zamulloa, 1990). The arid climate in a hydrographic basin is related to a slow recharge regime (Foster *et al*., 2003); therefore, it is essential to study precipitation and its relationship with the morphometry of the sub-basins as a product of long-term recharge. The average annual rainfall in the region is relatively low. In this sense, a map of the isohyets of the Caplina basin was prepared with data from the National Meteorology and Hydrology Service of Peru (Senamhi), interpolating 25 meteorological stations in the southern region.

Additionally, six representative stations were selected within the basin, and the variability of monthly mean precipitation is plotted through histograms.

Likewise, Zomlot, Verbeiren, Huysmans, and Batelaan (2015) postulated that the recharge and surface flow variation conditions were influenced by the topography, slope, drainage area, precipitation, temperature, evapotranspiration, percentage of sand in the soil, and the type of land use. The morphometric parameters were calculated by recharge indices and flow indices to characterize the sub-basins hydrology.

Morphometric characterization and analysis

Strahler (1957) proposed morphometric analysis as complementary to precipitation analysis to predict the basin geometry effect on complex physical processes and hydrological behavior during the drought periods. The morphometry of a basin spatially organizes the deposits that control the duration of waterlogging (Mourier, Walter, & Merot, 2008). During the flow, the water produces physical (erosion) and chemical (hydration, hydrolysis, oxide reduction) weathering, causing the dissolution of the rocks (Pino *et al*., 2017; Catalan, 1981).

For the sectorized morphometric analysis, the Caplina basin was divided into nine tributary sub-basins: Honda, Magollo, Caplina, Uchusuma, Los Molles, Cauñani, Hospicio, Espíritus, and Escritos (Figure 1); using the digital elevation model (DEM) with a resolution of 12.5 m per pixel (Shuttle Radar Topography Mission, NASA).

The morphometric parameters were grouped into classes, with weights from 0 to 7. The value 0 indicates the lowest incidence, whereas the value 7 represents the highest incidence to recharge or water-rock contact.

Morphometric recharge indices

For the determination of the recharge indices, the morphometric parameters that allow identifying the drained areas with the highest recharge in a basin were selected; this provides evidence of its magnitude reflected in the shape of the basin and in the thousands of years in which these processes occurred.

Compactness Coefficient (*K_C*) relates the perimeter (P) of the basin with that of the theoretical circle of area (A) equivalent to the basin area (Gravelius, 1914):

$$K_C = 0.282 \frac{P}{\sqrt{A}}$$

According to Gaspari *et al*. (2012), K_C is closely related to the concentration times, and it classifies the shape of the basin (Table 1).

Table 1. Weighting by compactness coefficient classification (Gaspari et al., 2012; Ortiz, 2004).

Shape classification	K_c	Weight
Almost round to oval-round	1-1.25	4
Oval-round to oval-elongated	1.25-1.5	3
Elongated-oval to oblong-rectangular	1.5-1.75	2
Rectangular	1.75-2.25	1
	> 2.25	0

The compactness is directly related to the occurrence of floods. An elongated basin will be less likely to generate floods than a compact area with a higher form factor (Henao, 1988).

Elongation Ratio (*Re*) is a relation between the circle diameter of the equivalent basin area (*d*) and the máximum length of the main channel of the basin (*Lc*), as proposed by Schumm (1956):

$$Re = \frac{d}{Lc}$$

Values lower than unity imply elongated shapes (Tabla 2); small *Re* supports the elongated basin form (Jardí, 1985).

Table 2. Weighting by elongation ratio classification (Jardí, 1985).

Relation	*Re*		Form	Weight
Lc < *d*	< 1	< 0.25	Very elongated	0
		> 0.25	Elongated	1
Lc > *d*	= 1		Oval	2
Lc = *d*	> 1		Round	3

Curva hipsométrica represents the drained area as a function of the altitude of the basin surface. According to Strahler (1952a), the curve shape is associated with the ages of the rivers. Table 3 shows the values for the weighting of rivers according to their age from their hypsometric classification. The oldest channels will have greater weight as they are proportional to the historical recharge time.

Table 3. Weighting by the age of rivers from the shape of their hypsometric curve

River age	Weight

Young river	1
Mature river	2
Old river	3

Morphometric indices of surface flow velocity

These indices provide information on the speed of surface runoff (Strahler, 1952b; Camino *et al*., 2018). If the runoff velocity decreases, the flow has more significant contact with the lithofacies. Therefore, parameters that describe the surface and underground flow behavior were selected.

The average slope (S_c) influences the behavior of the main channel. The steeper basins respond more quickly to rainfall by increasing their flows (Horton, 1945). It is calculated with the following formula, where $\sum Li$ is the sum of the lengths of the contour lines (km), *E* the equidistance between unevenness curves (km), and A the surface of the basin (km^2):

$$S_c = 100 \times \frac{(\Sigma Li)(E)}{A}$$

The slope represents the variability of the reliefs classified by Ortiz (2004). The mountainous reliefs cause rapid transport of rock fragments by physical erosion (Pino *et al*., 2017), which causes a reduced time for complete chemical disintegration. Therefore, in Table 4, the slopes that favor the water-rock interaction are weighted with a higher value.

Table 4. The weighting of the relief according to average slope and type of relief, modified after Ortiz (2004).

Average slope (%)	**Type of relief**	**Weight**
0-3	Flat	7
3-7	Gentle	6
7-12	Moderately rugged	5
12-20	Hilly	4
20-35	Heavily rugged	3
35-50	Very heavily rugged	2

50-75	Steep	1
>75	Very steep	0

Drainage density (*Dd*) is established based on the total length of the watercourses in the basin (*Li*) and their total area (*A*) (Table 5):

$$Dd = \frac{\sum Li}{A}$$

Table 5. Weighting of drainage density after Delgadillo and Páez (2008).

Drainage net	**Drainage density (km^{-1})**		**Weight**
Short	< 1	< 0.5	3
		> 0.5	2
Moderate	1-2		1
High	> 2		0

Camino *et al*. (2018) point out that the runoff time is shorter for ion exchange between the flow and the geological formation for basins with higher drainage density.

Geological characterization

The flow stays longer in the soil; its salinity will be higher (Sánchez, 2017). However, the effect is relative. Water in contact with sodium chloride for a few hours will be more saline than another sample in contact with quartz for years; here, the importance of the geology of the terrain through which the underground flow passes.

In the northeast of the Caplina basin, NW-SE directional structural controls predominate as a result of the Andean deformation (Monge & Cervantes, 2000) the transversal distribution to the drainage of the Caplina basin (NE-S0), position the controls as a conditioning structure for the storage of water infiltrated by precipitation. The infiltration is directed by the Caplina lineament (NE-SW) towards a mixing zone of the tributary sub-basins (Figure 1), conditioned by the Molles-Magollo lineament.

The geological characterization describes the emergence of sub-basins formation with a greater tendency to chemical weathering (i.e., lithology, hydrogeochemical and hydrogeological variability). In Table 6 and Table 7, values are weighted based on lithological classification, storage properties, and qualitative measurement factors.

Table 6. According to the hydrogeological classification, the weighting of physical properties in the water-rock contact.

Hydrogeological classification	Porosity	Permeability	Water-rock contact	Weight
Aquitards	High	Low	High	3
Aquifers	High	High	Moderate	2
Aquiclutes	High	Very low	Moderate	1
Aquifuges	Very low	Very low	Low	0

Table 7. The weighting of origin and lithological classification.

Lithology and origin	Weight
Sedimentary volcanic/calcareous	3
Sedimentary alluvial	2
Plutonic	1
Metamorphic	0

Hydrogeological characterization

In the Caplina basin, intrusive outcrops that modify the permeability and hydrogeological behavior of the geological formations are related to the water-rock contact time due to the retention of the flow in the pores. According to the capacity to store water (property of porosity) and its permeability, geological formations are classified into aquifers, aquitards, aquicludes, and aquifuges (Custodio & Llamas, 1983; García & Fernández, 2009). Table 6 shows the weighting factor by hydrogeological classification and physical properties.

Geochemical characterization

The degree of water-rock interaction depends on a series of factors, such as hydraulic properties and local flow patterns, which are influenced by the lithology where the groundwater passes, highlighting the presence of alterable minerals and surface alteration; Table 7 shows the weighting according to the lithological origin of and geochemical composition.

Results

Hydrological behavior in morphometry

Figure 3 presents the precipitation histograms of six meteorological stations in the Caplina basin. The altitude of each station is also shown in the figure. The La Yarada station located in the basin delta is observed with very low to zero accumulated monthly precipitation (maximum peak of 1 mm during June). The basin's middle area register stations got 30 mm/year of rainfall. Palca and Toquela stations situated at a higher altitude in the basin recharge zone, with annual accumulated precipitation is (65-165 mm/year). In the middle and upper areas of the basin, the transcendental precipitation for the underground recharge of the basin occurs in the first months of the year (Figure 2).

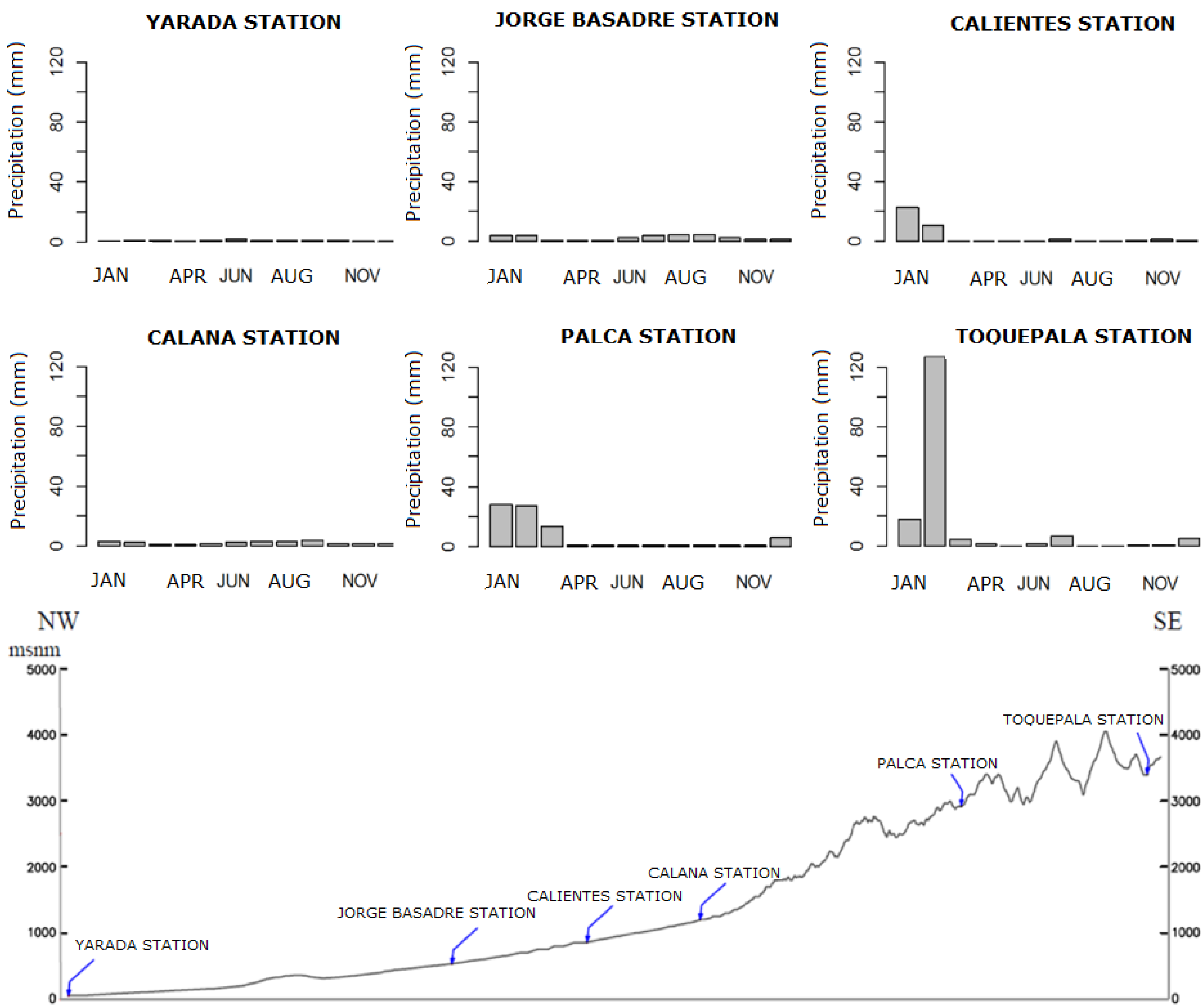

Figure 2. Precipitation histograms at representative stations in the basin during 2019-2020.

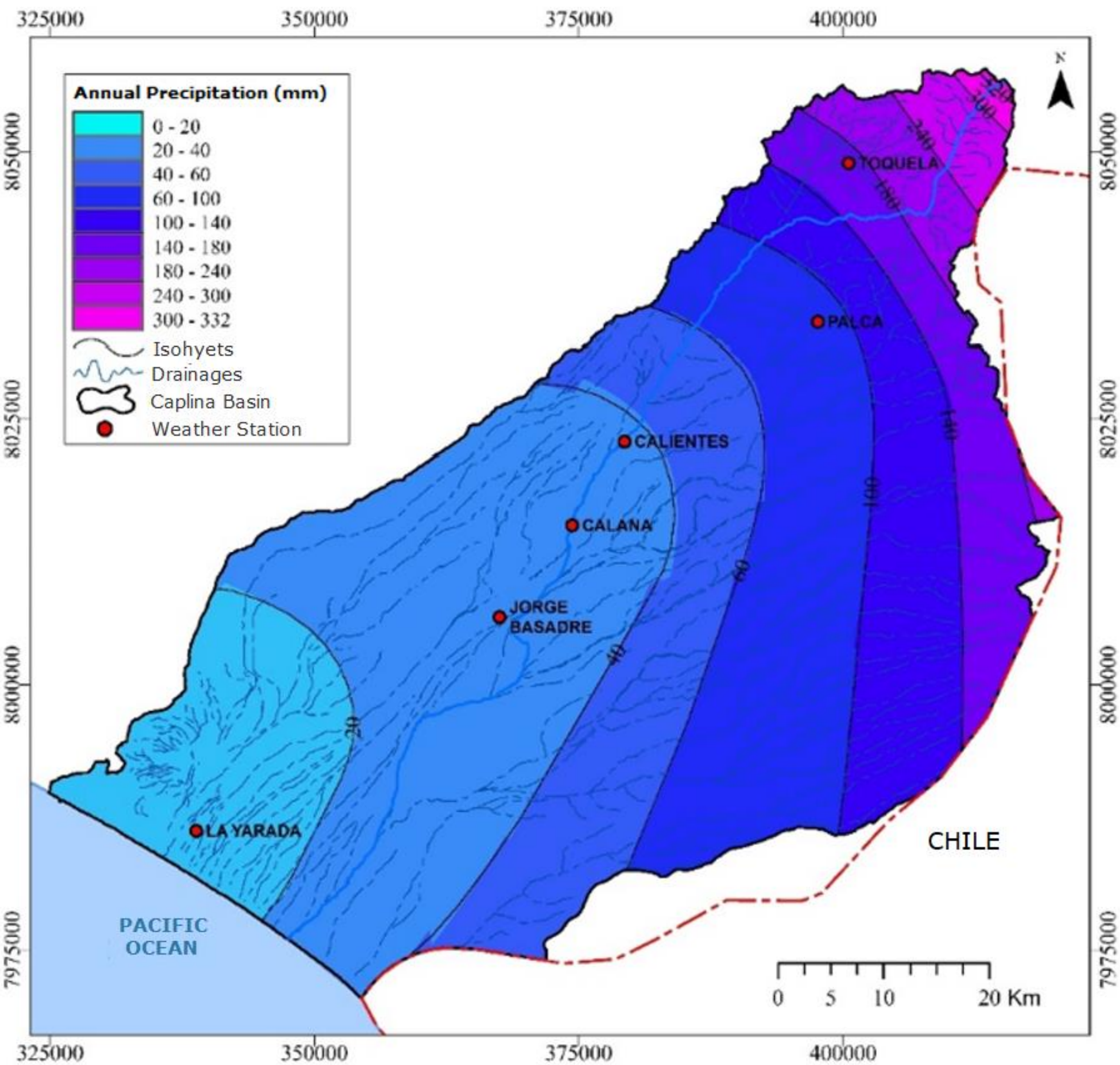

Figure 3. Precipitation isohyets in the Caplina basin.

In contrast, in the isohyets map (Figure 3), the annual precipitation varies between 0 and 330 mm. The strips with the highest recharge distribution are perpendicular to the tributary sub-basins NE-SW orientation to the Caplina basin. It is essential to have greater morphometric detail by sub-basin in this sense.

Sub-basin recharge

The compactness coefficient in the tributary sub-basins is more significant than 1.75, classifying them as elongated (Gaspari *et al*., 2012). The elongation ratio is less than unity, which confirms that the shape of the sub-basins is elongated (Jardí, 1985). In this sense, it is convenient to identify the highest values.

Figure 4 (a,b) shows the typical hypsometric curves for different river sizes and the Caplina basin. Strahler (1952a) classified the main channel of the Caplina basin as mature.

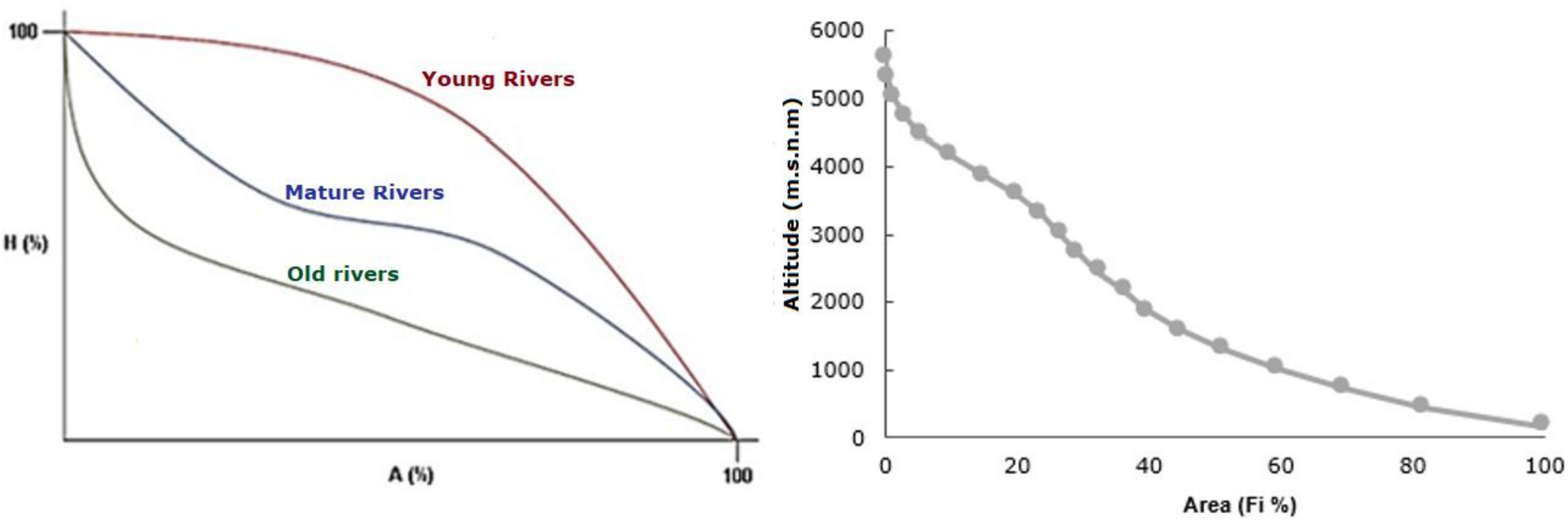

Figure 4. (a) Typical hypsometric curves (Strahler, 1952a); (b) Hypsometric curve of the Caplina basin.

Runoff velocity and contact time

The basin slope presents a general decreasing trend in the NE-SW direction. In the lower part of the basin (SW), between 0 and 1 000 masl, the slope is 3 %, representing a smooth relief, and in the upper part of (NE), between the heights 1 200 to 5 400 masl, it is 32 %, heavily rugged relief.

The weighting of the slopes is detailed in Table 8, which made it possible to differentiate the reliefs of the sub-basins, where the Magollo sub-basin of smooth relief stands out, while the other sub-basins with higher surface flow velocity as they are rugged and heavily rugged.

Table 8. The weighting of morphometric parameters against chemical weathering

		Morphometric parameters	Symbology	Units	Caplina basin	Sub-basins								
						Honda	Magollo	Caplina	Uchusuma	Los Molles	Cauñani	Hospicio	Espiritus	Escritos
Recharge rates	(i). shape of the basin	Compacity coefficient by Gravelius (1914)	K_C	-	1.83	3.82	2.17	2.23	2.26	2.61	2.20	2.62	1.99	2.44
		Classification of K_C by Gaspari (2012)	K_C	-	Elongated	Elongated	Elongated	Elongated	Elongated	Elongated	Elongated	Elongated	Elongated	Elongated
		Choose minors (value:1)	-	-	-	0	1	1	0	0	1	0	1	0

		Elongation ratio by Schumm (1956)	***Re***	-	0.70	0.24	0.44	0.39	0.39	0.33	0.40	0.34	0.40	0.34
		Clasification of Re by Jardí, (1985)	-	-	Elongated	Very Elongated	Elongated	Very Elongated	Very Elongated	Very Elongated	Very Elongated	Very Elongated	Very Elongated	Very Elongated
		Choose majors (value: 1)	-	-	-	0	1	1	1	0	1	0	1	0
	(ii). relief	Hypsometric curve Strahler, (1952a)	-	-	Mature rivers	Old rivers	Mature rivers	Mature rivers	Mature river	Young river	Young river	Young river	Mature river	Mature river
	(ii). relief	Weight with Table 2 (Strahler, 1952a)	-	-	-	3	2	2	2	1	1	1	2	2
Flow rates	**iii). Drainage network**	Middle slope (Horton, 1945)	S_c	%	27.02	21.19	10.57	37.78	32.83	27.02	30.39	33.78	37.67	34.80
Flow rates	**iii). Drainage network**	Classification of Sc by Ortiz (2004)	-	-	Heavily rugged	Heavily rugged	Medium rugged	Very heavily rugged	Heavily rugged	Heavily rugged	Heavily rugged	Heavily rugged	Very heavily rugged	Heavily rugged
Flow rates	**iii). Drainage network**	Weight with Table 3 (Ortiz, 2004)			3	3	5	2	3	3	3	3	2	2
Flow rates	**iii). Drainage network**	Drainage density (Camino *et al.*, 2018)	***Dd***	km/km²	0.72	0.56	0.61	0.45	0.58	0.42	0.60	0.54	0.56	0.46
Flow rates	**iii). Drainage network**	Classification of *Dd* by Delgadillo and Páez (2008)			Baja	Baja	Baja	Baja	Baja	Baja	Baja	Baja	Baja	Baja
Flow rates	**iii). Drainage network**	Choose minors (value: 1)			-	2	2	3	2	3	2	2	2	3
Weighting by sub-basin						8	11	9	8	7	8	5	8	7

The drainage density of the basin is 0.72 km^{-1}, representing a slow hydrological response. This relationship varies in the tributary sub-basins from 0.42 to 0.61 km^{-1}. The Caplina, Los molles, Espíritus and Escritos sub-basins present lower drainage densities.

According to the indices shown in Table 8, the weighting of the morphometric parameters supports the potential of the sub-basins to generate chemical weathering. Therefore, based on the results of Table 8, it is defined that the geological analysis will only be carried out for the Caplina and Magollo sub-basins because they present the highest scores, 9 and 11, respectively.

Geology and weathering in the Caplina sub-basin

In the Caplina sub-basin, most intrusives outcrop (Figure 5), generating hydrothermal alteration zones (Acosta, Alván, Mamani, Oviedo, & Rodríguez, 2010); weathering in these areas produces the dissolution of heavy chemical elements found in water. Also, in some springs, the minimum pH is 2.30 (Peña, Cotrina, & Acosta, 2009).

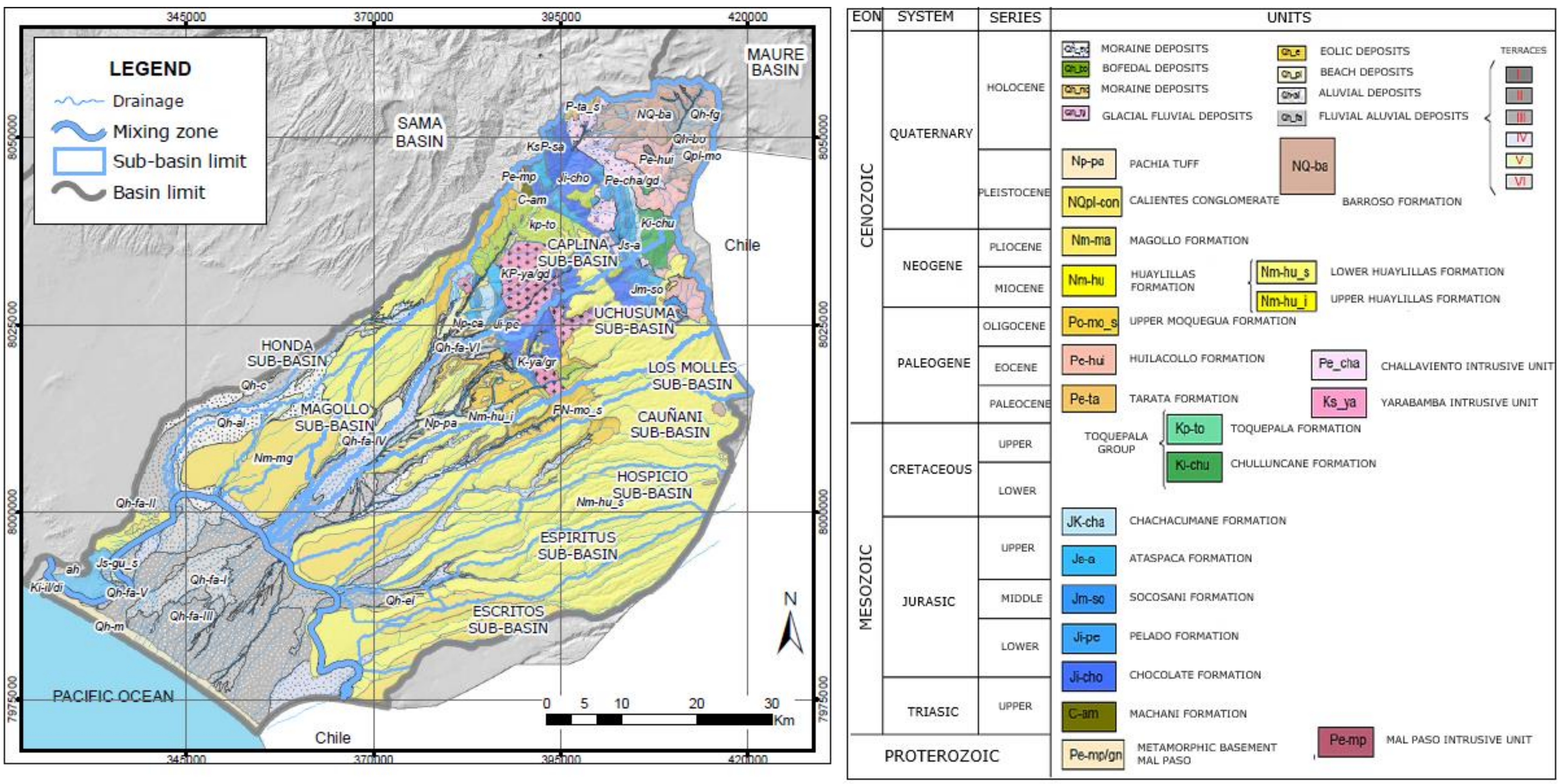

Figure 5. Geological and structural map of the Caplina basin at a scale of 1: 750,000 after Peña *et al*. (2009).

The outcropping geological formations in the Caplina Sub-basin are described below by age.

Mal Paso basement is made up of gneiss, granitic, and granodioritic orthogneiss; its metamorphic origin makes it little susceptible to alteration and weathering. It is superficially fractured, with low transmissibility, classified as an aquiclude, and low impact weighted to the salinization of the surrounding water.

Ambo Group is a sequence of conglomerates, black shales with calcareous sandstones. Calcite, feldspar, and plagioclase are prone to react on phyllosilicates. It behaves like a sedimentary fissured aquifer without surface alteration.

Junerata Formation is known as Volcánico Chocolate. It consists of andesitic lava spills and tuffs. Ferromagnesian minerals stand out from which it could be altered in Filosilicate (Chlorites). It presents superficial fractures and behaves like an aquitard.

Pelado Formation is made up of conglomerates, shales, and silicified limestone. The calcite coming from the shales will tend to dissolve in the erosive contact by the Caplina river; However, its silicified state would hinder any reaction and generate low permeability in fractures, classified as an aquitard.

San Francisco Formation is also denominated Socosani. It is made up of calcareous sandstones, conglomerates, and limestone. Its calcareous sedimentary nature is susceptible to calcite reaction. The waters circulating over this geological formation are crossed transversely by the Incapuquio fault, with high permeability. This unit corresponds to a sedimentary fissured aquifer.

Ataspaca Formation is a sequence of gray sandstones and dark shales with marl levels. Calcareous mineralogy, prone to dissolution. It is classified as a sedimentary fissured aquifer.

Chachacumane Formation is of gray quartzite sandstones with interspersed levels of shales. To be metamorphosed, the chemical reactions are focused on the hydrolysis of the superficial weak argillic alteration. In its outcrop, there are small upwellings of groundwater. It is classified as a highly fractured aquifer.

Chullucane Formation is a conglomerate of andesitic clasts and gravels. Plagioclase would be the most likely mineral to react. In addition, it presents weak argillic alteration. This sedimentary, volcanic formation behaves like a fissured aquifer.

Toquepala Formation is rhyolite and andesite interspersed with lenses of sandstones and conglomerates. It is classified as a fissured volcanic aquifer.

Tarata Formation is dominated by andesitic breccias and spills, with levels of sandstones and shales. It is classified as an aquitard due to the porosity of the tuffs, with a prolonged flow, conditioning a more significant contact with minerals typical of the volcanic environment.

Huilacollo Formation is of andesitic breccia, dacitic tuff and riodacitic. The water that flows over this geological formation contributes As, B, and Al from a geothermal source (Pino *et al*., 2017). The acidic composition of water reacts with plagioclase and feldspars. It is classified as a fissured aquifer.

Hot Conglomerado is polymictic conglomerates that make up an essential part of the valley fill. Therefore, their deposits record the fluvial dynamics of the region's rivers. These characteristics confer it as a double porosity, cracked, and porous aquifer.

Volcanic Barroso consists of tuffs and trachytic and andesitic composition lavas. It is interstratified with sediment banks and presents large areas of hydrothermal alteration, together with minerals of volcanic origin, rich in heavy elements that release Ca^{2+}, Na^{+}, As, B, and Al ions. They constitute the vital feeding and recharge zone of the Caplina Basin. It is classified as a volcanic fissured aquifer.

The intrusives that emerge in the Caplina sub-basin are described below.

Yarabamba Unit comprises plutonic rocks, granodiorite, and diorites, intruding on the Pelado and San Francisco sedimentary formations. (Wilson & García, 1962). They generate essential mineralizations with hydrothermal alteration. The permeability occurs by fracturing; in some old galleries that the intrusive Yarabamba crosses, there is a flow of 0.2 l/s. It is classified as an intrusive aquitard

Unidad Challaviento is made up of granodiorite and sienogranites. The intrusion of the rock body generates propylitic hydrothermal alteration and is classified as an intrusive aquitard.

Geology and weathering in the Magollo Sub-basin

The Magollo sub-basin presents the most remarkable predisposition to rock dissolution due to chemical weathering at low flow velocity. Descending geological formations in ancient times are described.

Moquegua Formation is made of silty sand conglomerates. Its sedimentary and porous nature classifies it as a fissured aquifer and is characterized by consolidated fluvial sediments with medium permeability, corresponding to a sedimentary aquifer.

Huaylillas Formation is pinkish, rhyolitic tuffs interspersed with thin layers of massive green sandstones. The permeability originates in its fractures, generating a potential dissolution zone. It is classified as a volcanic sedimentary aquitard.

Magollo Formation is of conglomerates and dark gray Feldspars sandstones. This porous sedimentary formation in the Magollo sub-basin is the most favorable for groundwater storage and is classified as a sedimentary porous fissured aquifer.

Susceptibility to chemical weathering

The geochemical and hydrogeological characteristics in the outcropping formations of the Caplina and Magollo sub-basins were described earlier. Table 9 presents a heuristical classification based on porosity,

Tecnología y Ciencias del Agua

OPEN ACCESS

Check for updates

permeability, and lithology. Tables (6 and 7) state the weightage of their influence on the water-rock contact.

Table 9. A qualitative classification of susceptibility to chemical weathering.

Sub-basin	Geological Formation	Lithology (Acosta *et al*., 2010)	Alterable minerals	Superficial alteration (Acosta *et al*., 2010)	Hydrogeological Classification (Peña *et al*., 2009)	Susceptibility to salinize
Caplina	Yarabamba intrusive unit	Granodiorite & diorites	-	Hydrothermal	Intrusive aquitard	High
		1	-	3	3	7
	Unidad intrusiva Challaviento	Granodiorite & senogranites		Hydrothermal propylitic	Intrusive aquitard	High
		1	-	3	3	7
	Basamento metamórfico Mal paso	Gneiss, granitic or granodioritic orthogneisss	-	-	Acuicludo	Low
		0	-	-	0	0
	Ambo Group	Conglomerates with quartz, black shales with calcareous sandstones	Calcite, Feldspars & Plagioclase	-	Fissured aquifer	Medium
		3	-	-	2	5
	Junerata Formation / Chocolate Volcanic	Basaltic Andesites & conglomerates	-	-	Sedimentary aquitard	Medium
		3	-	-	3	6
	Pelado Formation	Conglomerates, shales & silicified limestones	Calcite & quartz	-	Sedimentary aquitard	Medium
		2	-	-	3	5
	San Francisco / Socosani Formation	Calcareous sandstones, conglomerates & limestone	Calcite	-	Fissured aquifer	Medium
		3		-	2	5
	Ataspaca Formation	Gray sandstone and dark shales & marl layers	Calcite	-	Fissured aquifer	Medium
		3	-	-	2	5
	Chachacumane Formation	Gray quartzitic sandstone & shale layers	-	Weak Argillic	Fissured aquifer	High
		3	-	2	2	7

Sub-basin	Geological Formation	Lithology (Acosta *et al*., 2010)	Alterable minerals	Superficial alteration (Acosta *et al*., 2010)	Hydrogeological Classification (Peña *et al*., 2009)	Susceptibility to salinize
	Chullucane Formation	Conglomerates with andesitic clasts & gravitas	Plagioclase	Weak Argillic	Fissured aquifer	High
		3	-	2	2	7
	Toquepala Formation	Rhyolite and andesite with lenses of sandstones & conglomerates	Feldspar Plagioclase	-	Fissured aquifer	Medium
		3	-	-	2	5
	Tarata Formation	Andesitic breccia & spills with levels of sandstones and shales	Plagioclase	-	Aquitard	Medium
		3	-	-	3	6
	Huilacollo Formation	Andesitic breccia, riodacitic dacitic tuffs	Plagioclase Feldspar	Hydrothermal	Fissured aquifer	High
		3	-	3	2	8
	Hot Conglomerate	Polymictic conglomerates	-	-	Fissured aquifer	Low
		2	-	-	2	4
	Volcanic Barroso	Tufos & lavas trachytic and andesite	Plagioclase Feldspar	Hydrothermal sectorized	Fissured aquifer	High
		3	-	2	2	7
Magollo	Moquegua Formation	Silty sand conglomerates	-	-	Fissured aquifer	Low
		2	-	-	2	4
	Huaylillas Inferior Formation	Tobias, rhyolitic & riodacite	-	-	Aquitard	Medium
		3	-	-	3	6
	Magollo Formation	Conglomerates & dark gray sandstones	Feldspar	-	Fissured aquifer	Low
		2	-	-	2	4

Discussion

Morphometric and geological analysis

The morphometric weighting in the Caplina basin presents a different hydrological behavior, obtained individually for each tributary sub-basin (Table 8). The valuations in each of the nine tributary sub-basins are interpreted.

The increased weightings formed the Spirits and Writings sub-basins in the recharge indices; however, they are located in the driest area of the Caplina basin. Likewise, they decrease considerably in the hypsometric weighting curve. So, the age of the channel differs in the historical weighting recharge. The flow velocity indices give greater weight to the Magollo, Los Molles, Hospicio, and Escritos sub-basins due to the slow hydrological response, generating more residence time for chemical reactions. The Uchusuma sub-basin is the second-best weighted in recharge rates; however, it has a higher flow velocity that causes erosion and sediment transport, but not chemical weathering. The contrast of the recharge and velocity indices in the final weighting makes it possible to identify the Caplina and Magollo sub-basins with the most favorable conditions for chemical weathering.

The isohyet map delimits low mean annual precipitation in the Magollo sub-basin. However, the morphometric parameters indicate a higher recharge, infiltrated in the Moquegua formation until the Huaylillas volcanic event (lower Miocene, 25.3 ± 0.8 Ma). The pyroclastic material overlies the Moquegua formation. Likewise, we can infer that the average precipitation has decreased in the last 50 years, a period in which records are available in the meteorological stations of the region.

The models of Pacheco & Van der Weijden (Pacheco & Van der Weijden, 2012; Pacheco & Van der Weijden, 2014) and Rajbanshi and Bhattacharya (2020) apply equations and algorithms to estimate erosion rates by flow with a circulation of 1.4 to 2.8 years. However, the hyper-arid climate in the Caplina basin can generate a circulation time of 100 to 10,000 years and experience a moderate amount of weathering (Kanhaiya *et al*., 2019; Foster *et al*., 2003).

The qualitative weighting of the geology in Table 9 identifies hydrogeological units classified into three levels, whose degree of susceptibility to chemical weathering varies between High to Low and negligible for the outcropping formations in sub-basins less favorable for weathering. The initial analysis of the Susceptibility Map (Figure 6) shows us that the areas of most significant susceptibility are transversal to the main river in the basin, Río Caplina, and the drainage of the streams:

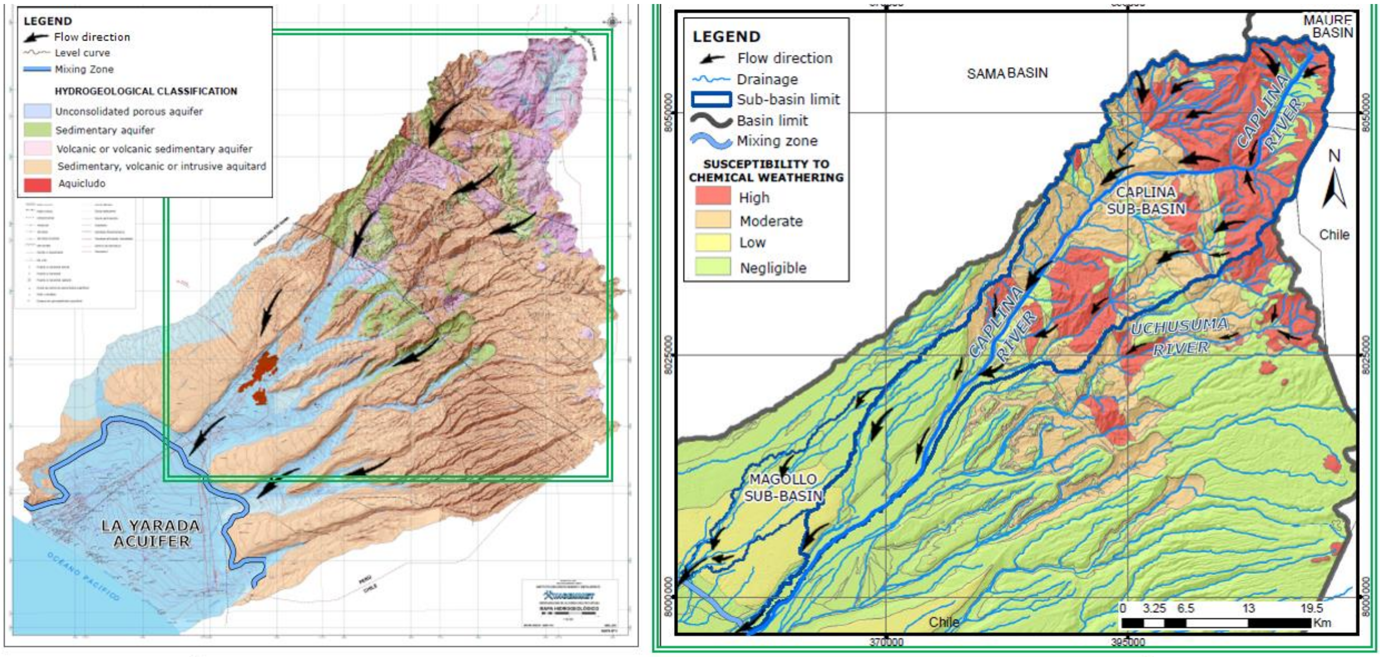

DEGREE OF SUSCEPTIBILITY TO CHEMICAL WEATHERING	
	HIGH SUSCEPTIBILITY (7 or more): Hydrothermalism in fissured aquifers and aquitards of intrusive origin, saturated, the greatest reaction occurs in altered areas.
	MEDIUM SUSCEPTIBILITY (5-6): Calcareous and sodium influence in volcanic aquitards and fissured aquifers with little permeability, favoring water-rock interaction in the pores of hydrogeological units.
	LOW SUSCEPTIBILITY (0-4): Alluvial fissured aquifers with favorable discontinuities for groundwater flow. Unconsolidated deposits that favor sediment transport, but not chemical reactions.
	NEGLIGIBLE SUSCEPTIBILITY: Areas that receive low recharge and precipitation. where there are no signs of surface alteration.

Figure 6. (a) Hydrogeological map of the Caplina basin after Peña *et al*. (2009); (b) susceptibility map to chemical weathering in the Caplina basin recharge zone.

These units generate salinization with underground flow directed to the SW that recharges the La Yarada aquifer (Figure 6). Pino *et al*. (2019a) found it in the high electrical conductivity map of the Yarada aquifer. It will be further studied in the hydrogeochemical analysis.

Hydrogeochemical analysis

In the works of Pacheco & Van der Weijden (Pacheco & Van der Weijden, 2012; Pacheco & Van der Weijden, 2014), Adhami and Hamidreza (2016), Kanhaiya *et al*. (2019), Rajbanshi and Bhattacharya (2020), they proposed evaluation factors of susceptibility to weathering without considering superficial alterations. In Table 9, the geological formations of high and medium susceptibility are differentiated by the weighting of the hydrothermal alteration.

The classification carried out in this work is validated by the hydrogeochemical study carried out by Peña *et al*. (2009) in 34 groundwater and surface water samples in the Caplina basin (Table 10, Table 11, and Table 12). Li *et al*. (2019) proposed an ion mass balance to calculate the dissolved charge using empirical equations. The proportion of the chemical composition of anions and cations is represented in the Piper Diagram. Such a diagram also allows differentiating the degree of interaction through ionic relationships related to the hydrogeological units where the samples were taken (Figure 7 and Figure 8).

Table 10. Calcium sulfate family in the Caplina basin after Peña et al. (2009).

Source	Sampling point	Sub-basin	Local geology	Water type	Dominant geological formation	Hydrogeological unit
River	Represa Paucarani	Maure	Fluioglacial Deposit	Ca-Mg-Na-SO_4		GEOTHERMAL
River	Canal Uchusuma (C Blanco)	Uchusuma	Q-fa, Chocolate, Yarabamba	Ca-Mg-Na-SO_4	Yarabamba	Intrusive aquitard
River	Río Uchusuma (Sector Higuerani)	Uchusuma	Socosani, Chocolate, Yarabamba	Ca-Na-Mg-SO_4		
River	Túnel Uchusuma	Uchusuma	Huilacollo	Ca-Mg-Na-SO_4	Huilacollo	Fissured aquifer
Spring	Paso de los Vientos	Uchusuma	Huilacollo, Huaylillas	Ca-Mg-Na-SO_4-HCO_3		
Spring	Captación Ataspaca	Caplina	Ataspaca, Chachacumane	Ca-Mg-SO_4	Chachacumane	Fissured aquifer
Spring	Captación Palca – Consumo	Caplina	Ataspaca, Socosani, Chachacumane	Ca-Mg-SO_4-HCO_3		
Spring	Quebrada Toquela	Caplina	Challaviento, Huilacollo, Barroso	Ca-Mg-SO_4	Challaviento / Huilacollo	Intrusive Aquitard Fissured Aquifer

Source	Sampling point	Sub-basin	Local geology	Water type	Dominant geological formation	Hydrogeological unit
Spring	Manante Aruma	Caplina	Huilacollo, Barroso, Huaylillas	$Ca\text{-}Na\text{-}Mg\text{-}SO_4\text{-}Cl$	Huilacollo/ Barroso	Fissured aquifer
Spring	Manantial Pampa Soroche	Caplina	Qpl-morrenas, Barroso	$Ca\text{-}Na\text{-}Mg\text{-}SO_4\text{-}HCO_3$		
River	Captación Caplina	Caplina	Chachacumane, Socosani, Ataspaca	$Ca\text{-}Na\text{-}SO_4\text{-}Cl$	Chachacumane	
River	Río Caplina Parte baja	Caplina	Toquepala, Challaviento, Yarabamba	Ca-Na-SO4	Challaviento/ Yarabamba	Intrusive aquitard
Spring	Captación Palca – Agro	Caplina	Chocolate, Socosani, Toquepala, Challaviento	$Ca\text{-}SO_4\text{-}HCO_3$	Challaviento	
Spring	Manante Ataspaca	Caplina	Huaylillas and Toquepala	$Ca\text{-}Na\text{-}SO_4\text{-}Cl$	Huaylillas	Volcanic aquitard
Underground well	Quebrada Ancopuja	Uchusuma	Huaylillas	$Ca\text{-}Na\text{-}SO_4\text{-}HCO_3$		
Underground well	IRHS - 220 Las Palmeras	Zona Mezcla	Q-fa	$Ca\text{-}Na\text{-}SO_4\text{-}Cl$		Alluvial
Underground well	IRHS - 146 Cooperativa 60	Zona Mezcla	Q-fa	$Ca\text{-}Na\text{-}Mg\text{-}SO_4\text{-}Cl$		Alluvial
River	Quebrada Humalata	Caplina	Tarata	$Ca\text{-}SO_4$	-	Sedimentary
River	Quebrada Piscollane	Caplina	Barroso, Qh- bofedal, Q-fa	$Ca\text{-}SO_4$	Barroso	Fissured aquifer
Spring	Manante Cocavira	Caplina	Huilacollo and Qh-bofedal	$Ca\text{-}SO_4$	Huilacollo	
Spring	Manantial Tirata	Caplina	Huilacollo	$Mg\text{-}Ca\text{-}SO_4$		

Table 11. Sodium chloride and calcium chloride family in the Caplina basin after Peña et al. (2009).

Code	Sampling point	Sub-basin	Local geology	Water type	Dominant geological formation	Hydrogeological unit
Spring	Captación "D" Cauñani	Cauñani	Q-fa, Huaylillas, Pachia	$Na\text{-}Ca\text{-}Cl\text{-}HCO_3$	Huaylillas	Volcanic aquitard
Manantial	Captación "C" Cauñani	Cauñani	Q-fa,Huaylillas, Pachia	$Na\text{-}Ca\text{-}Cl\text{-}HCO_3$		
Underground well	IRHS - 024 La Esperanza	Zona Mezcla	Q-fa, Huaylillas, Chocolate (Guaneros)	$Na\text{-}Ca\text{-}Cl\text{-}SO_4$	Huaylillas	
Spring	Manante Termal Calientes	Caplina	Chachacumane, Socosani, Ataspaca	$Na\text{-}Ca\text{-}Cl\text{-}SO_4$	Chachacumane	Fissured aquifer

Spring	Aguas Termales Aruma	Caplina	Huilacollo, Barroso, Huaylillas	Na-SO_4-Cl	Huilacollo/ Barroso	
Underground well	IRHS - 112 La Yarada	Zona Mezcla	Fluvial-alluvial Dep. (Q-fa)	Na-Ca-SO_4-Cl		Alluvial with Marine Intrusion
Underground well	IRHS - 054 Velasco Alvarado	Zona Mezcla	Fluvial-alluvial Dep. (Q-fa))	Ca-Na-Cl-SO_4		
Underground well	IRHS - 051 Los Palos	Zona Mezcla	Fluvial-alluvial Dep. (Q-fa)	Ca-Na-Cl-SO_4		

Table 12. Calcium bicarbonate family in the Caplina basin after Peña et al. (2009).

Code	Sampling point	Sub-basin	Local geology	Water type	Dominant geological formation	Hydrogeological unit
Spring	Manante Yangane	Uchusuma	Chulluncane	Ca-Cl-HCO_3	Chulluncane	Fissured aquifer
Spring	Manante Piscollane	Caplina	Huilacollo, Barroso	Ca-Mg-Na-HCO_3	Huilacollo, Barroso	
Spring	Quebrada Quilla	Caplina	Chulluncane, Challaviento	Ca-Mg-HCO_3-SO_4	Challaviento	Intrusive aquitard
Spring	Quebrada Coapalca	Uchusuma	Moquegua, Huaylillas	Ca-Na-HCO_3-SO_4	Huaylillas	Volcanic aquitard
Spring	Quebrada Haquimanqui	Uchusuma	Toquepala, Moquegua, Huaylillas	Ca-Na-HCO3-SO_4		

Tecnología y Ciencias del Agua

OPEN ACCESS

Check for updates

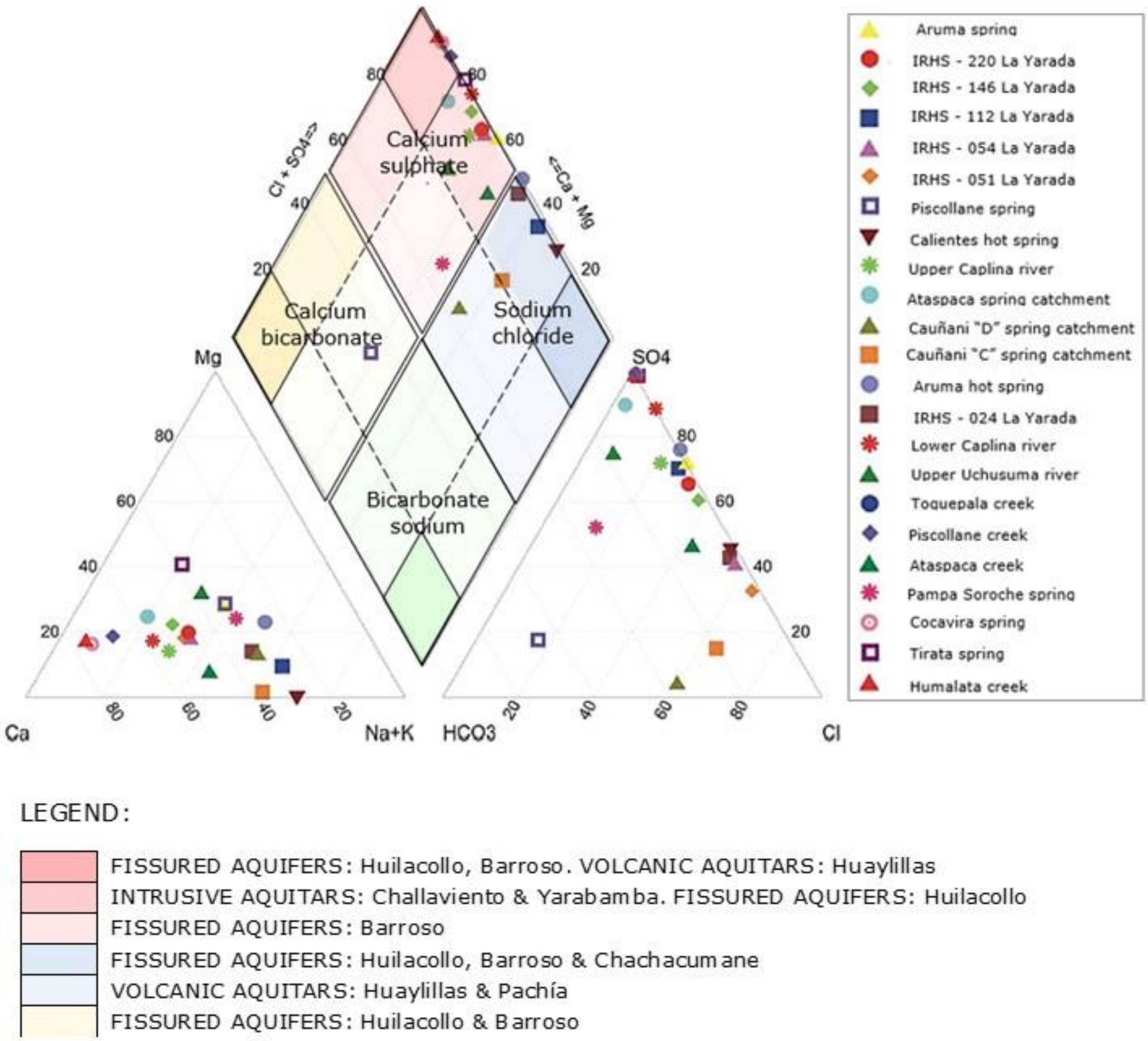

Figure 7. Piper diagram in the Caplina sub-basin after Peña *et al*. (2009).

Tecnología y Ciencias del Agua

OPEN ACCESS

Check for updates

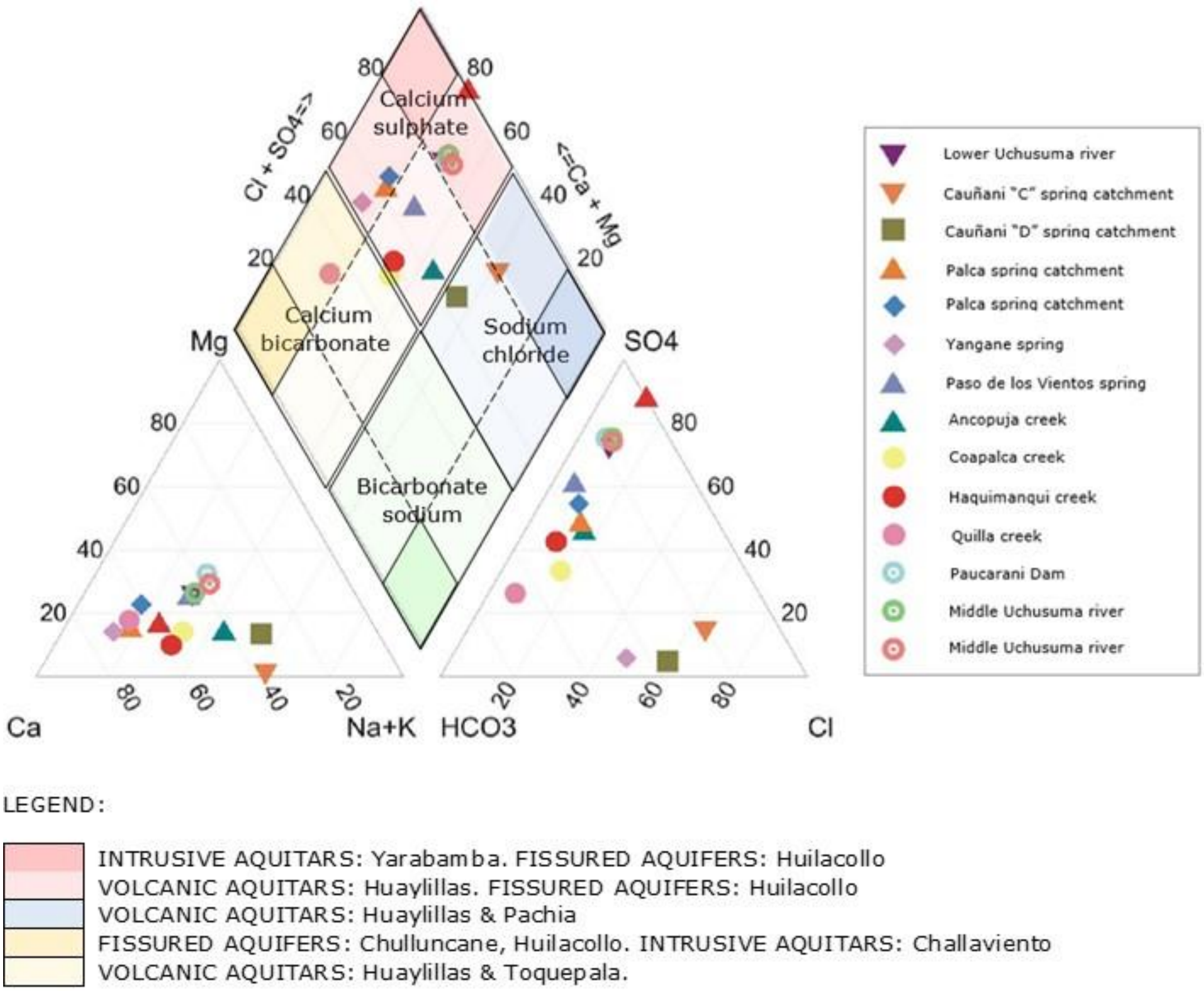

Figure 8. Piper diagram in the Uchusuma and Cauñani sub-basins after Peña *et al*. (2009).

The geochemical facies of the main surface and groundwater sources in the Caplina sub-basin (Figure 7) experience spatially polarized ion exchange. In contrast, in the Uchusuma and Cauñani sub-basins (Figure 8), it is observed that they retain certain neutrality, corroborating the presence of sediment transport with an erosive tendency in the Uchusuma sub-basin, but not chemical weathering.

Peña *et al*. (2009); Vera, Pino-Vargas, Verma, Chucuya, Chávarri, Canales, Torres-Martínez, Mora, Mahlknecht (2021), identify four geochemical facies in surface and underground water sources in the Caplina basin, regrouping into three due to the predominance of anions and their relationship with the emerged geological environment.

Group I: Calcium-sulfated

The dominant family in the basin is the calcic-sulfated one. Sulfates come from the oxidation of sulfides due to hydrothermal alteration in the mineral occurrences of the intrusive Yarabamba and Challaviento (Acosta *et al*., 2010). On the surface of fissured aquifers: Huilacollo and Barroso, the hydrothermal alteration extends in-depth, arising in catchments and springs. In this sense, the weighting of the surface alteration was mapped by Acosta *et al*. (2010) (Table 9). Meanwhile, Ca^{2+} ions are released due to chemical reactions in calcareous sedimentary formations, such as Ataspaca.

Group II: Sodium–chloride, and calcium–chloride

The chloride anions come from the Aruma and Calientes hot springs in the outcrops of Huilacollo, Barroso, and Chachacumane, which were predominated in the deep waters of the Borateras geothermal field (Vargas *et al*., 2012). The geochemistry of the geothermal reservoirs of the South volcanic axis encompassed the part of the Caplina basin.

Likewise, there was a considerable influence of Na^+ and Ca^{2+} from the Huaylillas formation. An increase in reactions was observed in volcanic aquitards with high porosity, despite receiving little precipitation.

Group III: Calcium bicarbonate

Calcium-bicarbonate sources represent the ideal composition of andesitic volcanic rocks (Ng, 2015) located in the fissured aquifers of Huillacollo, Barroso, and Chulluncane. In mixing groundwater, meteoric and glacier water, they generate seasonal variation in the hydrochemistry of the basins (Ansari *et al*., 2019; Chucuya, Vera, Pino-Vargas, Steenken, Mahlknecht, Montalván, 2022). The bicarbonate anion would come from a concise path of local flow. They are related to the reaction of CO_2 coming from the soil's pores.

The characterization of the three groups is described in Tables 10, 11, and 12. The source type of the sampling point is related to the local geology and type of water to identify the dominant geological formation in the mineralization of the water. In this way, the hydrogeological unit corresponds to the hydrogeological behavior of the dominant geological formation.

79.41 % of the samples evaluated are connected with hydrogeological units classified as high and medium susceptibility (Table 9). This high correspondence validates the correct proposed classification. In addition, it was found that fissured aquifers influence 41.2 % of the total samples with hydrothermal alteration, predisposing ion exchange. 20.6 % of these samples outcrop in volcanic aquitards without considerable ionic exchange, and 17.6 % correspond to intrusive aquitards with a surface alteration.

Conclusions

The weighting methodology allowed to generate of the susceptibility map to chemical weathering, with 79 % validation of the hydrogeochemistry of the basin. Three hydrogeological units stand out in the Caplina basin: (1) fissured aquifers with hydrothermal alteration in the Huilacollo, Barroso volcanic, Chulluncane, and Chachacumane formations; (2) intrusive aquitards with hydrothermal alteration in the Yarabamba and Challaviento units; (3) aquitards of volcanic and porous origin in the Huaylillas formation.

In the hydrogeochemical analysis of water facies, the sulfate anion predominance originated from the oxidation of sulfides due to the mineral occurrences of Cu and Ag associated with intrusive aquitards. The pattern associated with greater susceptibility is the presence of hydrothermal alteration. The calcium and sodium facies resulted from chemical reactions in altered fissured aquifers and flow in calcareous sedimentary formations. Likewise, the reactions are intensified in the entrapment of the aquitards of the Huaylillas formation.

The geological formations studied emerge in the Caplina and Magollo sub-basins based on a heuristic selection in the morphometric parameters of all the tributary sub-basins to the Caplina basin. This methodology makes it possible to identify the characteristics of the sub-basins with the highest historical recharge. They have an oblong shape with a compactness coefficient (> 2.25) and an elongation ratio (> 0.39), the hypsometry of mature and old basins. The sub-basins with lower flow velocity have low slopes (3 %-12 %), with drainage density < 0.8 km^{-1}.

These parameters establish a basis for a classification weight of susceptibility to chemical weathering in an arid basin.

Acknowledgments

This work was developed within the framework of the research project, "Integration of hydrodynamic, hydrochemical and isotopic methods to specify the operation and sustainable management of the La Yarada aquifer, Tacna, Peru," founded by "Fondos de canon, sobrecanon y regalías mineras de la Universidad Nacional Jorge Basadre Grohmann, Tacna, Perú." In addition, we would like to thank Dr. Alfonso Aragón, head of the Geothermal Energy Department, National Institute of Electricity and Clean Energy of Cuernavaca, Mexico, for allowing the first author to stay at the facilities to carry out this research. The manuscript is significantly improved with comments and suggestions from anonymous reviewers.

References

Acosta, H., Alván, A., Mamani, M., Oviedo, M., & Rodríguez, J. (2010). Geología de los cuadrángulos de Pachía (36-v) y Palca (36-x), escala 1:50 000. Siete mapas. I*NGEMMET, Boletín, Serie A: Carta Geológica Nacional*, 139, 100.

Adhami, M., & Hamidreza, S. (2016). Sub-watershed prioritization based on sediment yield using game theory. *Journal of Hydrology*, 541(B), 977-987. Recovered from https://doi.org/10.1016/j.jhydrol.2016.08.008

ANA, Autoridad Nacional del Agua. (2011). *Informe técnico 003-Calidad de agua, cuenca Caplina-Tacna*. Tacna, Perú: Dirección de Gestión de Calidad de los Recursos Hídricos.

Ansari, Z., Ahmad, S., & Khan, M. A. (2019). Seasonal variations of streams hydrochemistry and relationships with morphometric/landcover parameters in the Bhagirathi Watersheds, Garhwal Himalaya, India. *Journal of the Geological Society of India*, 94(5), 493-500. Recovered from https://doi.org/10.1007/s12594-019-1346-y

Bransford, J., & Stein, B. (1987). *Trad cast: solución ideal de problemas*. Madrid, España: Labor.

Camino, M., Bó, M., Cionchi, J., López-de-Armentia, A., Del-Río, J., & De-Marco, S. (2018). Estudio morfométrico de las cuencas de drenaje de la vertiente sur del sudeste de la provincia de Buenos Aires (Argentina). *Revista Universitaria de Geografía*, 27(1), 73-97.

Catalan, L. J. (1981). *Química del agua* (2a ed.). Madrid, España: Talleres Gráficos Alonso.

Chucuya, S.; Vera, A.; Pino-Vargas, E.; Steenken, A.; Mahlknecht, J.; Montalván, I. Hydrogeochemical Characterization and Identification of Factors Influencing Groundwater Quality in Coastal Aquifers, Case: La Yarada, Tacna, Peru. Int. J. Environ. Res. Public Health 2022, 19, 2815. https://doi.org/10.3390/ijerph19052815

Custodio, E., & Llamas, M. (1983). *Hidrología subterránea*. Tomo I y II. Barcelona, España: Ediciones Omega.

Delgadillo, A., & Páez, G. (2008). Aspectos hidrológicos, subcuencas susceptibles a crecidas, escenarios de riesgo. En: Ferrer, C., & Duarte, M. (eds.). *Plan de desarrollo urbano del Municipio Antonio Pinto Salinas, bajo el enfoque de gestión del riesgo. Caracterización del riesgo de la cuenca del valle Mocoties*. Mérida, Venezuela: Fundación para la Prevención del Riesgo Sísmico (Fundapris).

Foster, S., Tuinhof, A., Kemper, K., Garduño, H., & Nanni, M. (2003). *Characterization of Groundwater Systems - key concepts and frequent misconceptions*. GW-MATE Briefing Note Series 2, Washington, D.C., USA: World Bank.

García M., & Fernández, A., (2009). *Hidrogeología básica. Las aguas subterráneas y su flujo* (3ª ed.). Madrid, España: Ediciones FIEC.

Garreaud, R. D., Molina, A., & Farias, M. (2010). Andean uplift, ocean cooling and Atacama hyperaridity: A climate modeling perspective. *Earth and Planetary Science Letters*, 292(1-2), 39-50. Recovered from https://doi.org/10.1016/j.epsl.2010.01.017.

Garreaud, R., Vuille, M., & Clement, A. C. (2003). The climate of the Altiplano: Observed current conditions and mechanisms of past changes. *Palaeogeography, Palaeoclimatology, Palaeoecology*, 194(1-3), 5-22. Recovered from https://doi.org/10.1016/S0031-0182(03)00269-4

Gaspari, F. J., Rodríguez-Vagaría, A. M., Senisterra, G. E., Denegri, G., Delgado, M. I., & Besteiro, S. (2012). Caracterización morfométrica de la cuenca alta del río Sauce Grande, Buenos Aires, Argentina. *Revista Electrónica del Comité de Medio Ambiente. AUGMDOMUS*, 4, 143-158. Recovered from https://revistas.unlp.edu.ar/domus/article/download/476/505/

Gravelius, H. (1914). *Morphometry of drainage bassins*. Amsterdam, The Netherlands: Elsevier.

Henao, J. (1988). *Introducción al manejo de cuencas hidrográficas*. Bogotá, Colombia: Universidad Santo Tomás.

Horton, R. E. (1945). Erosional development of streams and their drainage basins: Hydrophysical approach to quantitative morphology. *Bulletin of the Geological Society of America*, (56), 275-370.

Jardí, M. (1985). Forma de una cuenca de drenaje. Análisis de las variables morfométricas que nos la definen. *Revista de Geografía*, (19), 41-68.

Kanhaiya, S., Singh, B. P., Singh, S., Mittal, P., & Srivastava, V. K. (2019). Morphometric analysis, bedload sediments, and weathering intensity in the Khurar River Basin, central India. *Geological Journal*, 54(1), 466-481. Recovered from https://doi.org/10.1002/gj.3194

Li, X., Han, G., Liu, M., Yang, K., & Liu, J. (2019). Hydro-geochemistry of the river water in the Jiulongjiang River Basin, Southeast China: Implications of anthropogenic inputs and chemical weathering. *International Journal of Environmental Research and Public Health*, 16(3). Recovered from https://doi.org/10.3390/ijerph16030440

Manfreda, S., Nardi, F., Samela, C., Grimaldi, S., Taramasso, A., Roth, G. & Sole, A. (2014). Investigation on the use of geomorphic approaches for the delineation of flood prone areas. *Journal of Hydrology*, 517, 863-876. Recovered from https://doi.org/10.1016/j.jhydrol.2014.06.009

Molina, M. (2005). *Estudio de la intrusión salina en acuíferos costeros: sector Costa Quebrada Los Choros, IV Región*. Santiago de Chile, Chile: Universidad de Chile.

Monge, R., & Cervantes, J. (2000). *Memoria explicativa de la Geología del Cuadrángulo de Pachía y Palca* (36-v). Lima, Perú: Instituto Geológico Minero y Metalúrgico.l

Motta-Zamulloa, E. (julio, 1990). Agua y conflictos en el valle del Caplina (Tacna) siglos XVI-XIX. *Boletín de Lima*, (70). Recovered from https://boletindelima.pe/products/199070

Mourier, B., Walter, C., & Merot, P. (2008). Soil distribution in valleys according to stream order. *CATENA*, 72(3), 395-404. Recovered from https://doi.org/10.1016/j.catena.2007.07.012

Narvaez-Montoya, C., Torres-Martínez, J. A., Pino-Vargas, E., Cabrera-Olivera, F., Loge, F., & Mahlknecht, J. (2022) Predicting adverse scenarios for a transboundary coastal aquifer system in the Atacama Desert (Peru/Chile). *Science of The Total Environment*, 806, Part 1. Recovered from https://doi.org/10.1016/j.scitotenv.2021.150386

Ng, W. (2015). *Estudio hidrogeológico de la parte alta de la cuenca del río Ilo-Moquegua* (tesis Ingeniero Geólogo). Universidad Nacional San Antonio Abad del Cusco, Perú.

Ortiz, O. (2004). Evaluación hidrológica. *Hidrrored*, (1), 1-7.

Pacheco, F., & Van der Weijden, C. (2014). Role of hydraulic diffusivity in the decrease of weathering rates over time. *Journal of Hydrology*, 512, 87-106. Recovered from http://dx.doi.org/10.1016/j.jhydrol.2014.02.041

Pacheco, F., & Van der Weijden, C. (2012). Integrating topography, hydrology and rock structure in weathering rate models of spring watersheds. *Journal of Hydrology*, 428-429. Recovered from http://dx.doi.org/10.1016/j.jhydrol.2012.01.019

Peña, F., Cotrina, G., & Acosta, H. (2009). Hidrogeología de la cuenca del río Caplina. *Boletín 1*, *INGEMMET*. Recovered from https://repositorio.ingemmet.gob.pe/handle/20.500.12544/368

Pino, E. (2019). The La Yarada coastal aquifer, after 100 years of exploitation as a sustenance for agriculture in arid zones: A historical review. *Idesia*, 37(3), 39-45. Recovered from https://doi.org/10.4067/S0718-34292019000300039

Pino, E., Ramos, L., Mejía, J., Chávarri, E., & Ascensios, D. (2020). Medidas de mitigación para el acuífero costero La Yarada, un sistema sobreexplotado en zonas áridas. *Idesia (Arica)*, 38(3), 21-31. Recovered from https://doi.org/10.4067/s0718-34292020000300021

Pino, E., Montalván, I., Vera, A., & Ramos, L. (2019a). Stomatal conductance and its relationship with leaf temperature and soil moisture in olive cultivation (*Olea europaea* L.), in the period of fruit ripening, in arid zones. La Yarada, Tacna, Perú. *Idesia*, 37(4), 55-64. Recovered from https://doi.org/10.4067/S0718-34292019000400055

Pino, E., Ramos, L., Avalos, O., Tacora, P., Chávarri, E., Angulo, O., Ascensios, D., & Mejía, J. (2019b). Factors affecting depletion and pollution by marine intrusion in the La Yarada´s coastal aquifer, Tacna, Peru. *Tecnología y ciencias del agua*, 10(5), 177-213. Recovered from https://doi.org/10.24850/j-tyca-2019-05-07.

Pino, E., Chávarri, E., & Ramos, L. (2018). Governability and governance crisis its implications in the inadequate use of groundwater, case coastal aquifer of la yarada, Tacna, Perú. *Idesia*, 36(3), 77-86. Recovered from https://doi.org/10.4067/S0718-34292018005001301

Pino, E., Tacora, P., Steenken, A., Alfaro, L., Valle, A., Chávarri, E., Ascencios, D., & Mejía-Marcacuzco, J. A. (2017). Efecto de las características ambientales y geológicas sobre la calidad del agua en la cuenca del río Caplina, Tacna, Perú. *Tecnología y ciencias del agua*, 8(6), 77-99. Recovered from https://doi.org/10.24850/j-tyca-2017-06-06

Rajbanshi, J., & Bhattacharya, S. (2020). Assessment of soil erosion, sediment yield and basin specific controlling factors using RUSLE-SDR and PLSR approach in Konar River basin, India. *Journal of Hydrology*, 587, 124935. Recovered from https://doi.org/10.1016/j.jhydrol.2020.124935

Sánchez, F. (2017). *Hidrología superficial y subterránea*. Madrid, España: Createspace Independent Publishing Platform.

Secretaría de Gestión de Riesgos. (2015). *Propuesta metodológica para el análisis de amenaza por movimientos en masa*. Quito, Ecuador: Secretaría de Gestión de Riesgos.

Schumm, S. (1956). The evolution of drainage systems and slopes in badlands at Pearth Amboy, New Jersey. *Bulletin of the Geological Society of America*, (67), 597-646.

Strahler, A. (1957). Quantitative analysis of watershed geomorphology. *Transactions, American Geophysical Union*, 38, 913-920. DOI: 10.1029/TR038i006p00913

Strahler, A. (1952a). Hypsometric (area-altitude) analysis of erosional topography. *Bulletin of Geological Society of America*, (63), 1117-1142.

Strahler, A. (1952b). Hypsometrie analysis of erosional topography. *Bulletin of Geological Society of America*, (63), 923-938.

Vargas, V., Cruz, V., Antayhua, Y., Rivera, M., Chirif, H., & West, J. (2012). Estudio geotérmico campo Borateras. *INGEMMET. Boletín, Serie C: Geodinámica e Ingeniería Geológica,* 47, 74.

Vera, A.; Pino-Vargas, E.; Verma, M.P.; Chucuya, S.; Chávarri, E.; Canales, M.; Torres-Martínez, J.A.; Mora, A.; Mahlknecht, J. (2021). Hydrodynamics, Hydrochemistry, and Stable Isotope Geochemistry to Assess Temporal Behavior of Seawater Intrusion in the La Yarada Aquifer in the Vicinity of Atacama Desert, Tacna, Peru. Water 2021, 13, 3161. https://doi.org/10.3390/w13223161

Wilson, J., & García, W. (1962). *Geología de los cuadrángulos de Pachia y Palca Hoja 36v y 36x*. Lima, Perú: Instituto Geológico, Minero y Metalúrgico (INGEMMET)-Comisión de la Carta Nacional.

Zomlot, Z., Verbeiren, B., Huysmans, M., & Batelaan, O. (2015). Spatial distribution of groundwater recharge and base flow: Assessment of controlling factors. *Journal of Hydrology: Regional Studies*, 4, 349-368. Recovered from https://doi.org/10.1016/j.ejrh.2015.07.005